Molecular Recognition of cAMP by an RNA Aptamer†

Makoto Koizumi‡ and Ronald R. Breaker*

Department of Molecular, Cellular, and Developmental Biology, Yale University, P.O. Box 208103, New Haven, Connecticut 06520-8103

Received January 24, 2000; Revised Manuscript Received April 12, 2000

ABSTRACT: Two classes of RNA aptamers that bind the second messenger adenosine 3′,5′-cyclic monophosphate (cAMP; **1**) were isolated from a random-sequence pool using in vitro selection. Class I and class II aptamers are formed by 33- and 31-nucleotide RNAs, respectively, and each is comprised of similar stem−loop and single-stranded structural elements. Class II aptamers, which dominate the final selected RNA population, require divalent cations for complex formation and display a dissociation constant (K_D) for cAMP of ∼10 μM. A representative class II aptamer exhibits substantial discrimination against 5′- and 3′-phosphorylated nucleosides such as ATP, 5′-AMP, and 3′-AMP. However, components of cAMP such as adenine and adenosine also are bound, indicating that the adenine moiety is the primary positive determinant of ligand binding. Specificity of cAMP binding appears to be established by hydrogen bonding interactions with the adenine base as well as by steric interactions with groups on the ribose moiety. In addition, the aptamer recognizes 8,5′-*O*-cycloadenosine (**2**) but not N^3,5′-cycloadenosine (**3**), indicating that this RNA might selectively recognize the anti conformation of the *N*-glycosidic bond of cAMP.

Biological systems rely on various second messenger compounds in signal transduction pathways that are integral cellular determinants of both normal and disease states. For example, cAMP (Scheme 1, **1**) is a second messenger that is involved in cellular signaling processes that modulate protein phosphorylation (*1*). The concentration of cAMP inside cells is established by the function of various adenylate cyclases and cyclic nucleotide phosphodiesterases (PDEs). Adenylate cyclases are typically regulated by hormone stimulation, which induces the production of cAMP from adenosine 5′-triphosphate (ATP). In contrast, PDEs catalyze the hydrolysis of cAMP to produce adenosine 5′-monophosphate (5′-AMP), thereby reducing the signaling effect that is otherwise established by high cAMP concentrations. Intentional modulation of the activity of adenylate cyclases and PDEs is proving to be a promising strategy to achieve various therapeutic effects (*2*). Therefore, the development of additional means by which cAMP and other second messengers can be intentionally and discretely manipulated could be useful for the creation of new therapeutic strategies.

One possible strategy for the manipulation of cellular processes is the creation of novel enzymes and receptors. Recently, molecular engineers have begun employing combinatorial methods for macromolecular design to make new functional proteins and nucleic acids. For example, the process of SELEX has been used to isolate a myriad of RNA and DNA aptamers that serve as ligand-specific receptors (*3*−*5*). These aptamers can recognize a great diversity of small organic compounds such as dyes (*6*, *7*), amino acids (*8*−*10*), nucleotides (*11*, *12*), and aminoglycosides (*13*−*17*), among many other small and large molecules. Similarly, in vitro selection methods have been used to create numerous ribozymes and deoxyribozymes that catalyze chemical transformations, including phosphoester formation and cleavage reactions (*18*−*20*). The functional capabilities of nucleic acids perhaps could be exploited to create new receptors for cAMP that could be integrated into structures that detect the concentration of the second messenger in solution (*21*, *22*). In addition, novel catalytic nucleic acids that specifically recognize cAMP might be made to selectively destroy cAMP, thereby simulating the function of natural PDEs.

Scheme 1: The Target Ligand cAMP (**1**) and Its Immobilization on an Agarose Matrix via a 9-Atom Spacer to Position C8 of the Adenine Ring

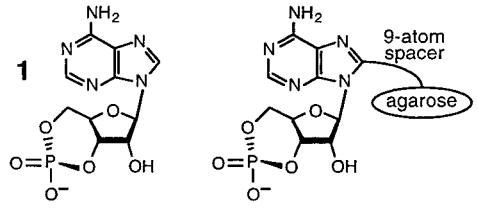

cAMP **cAMP agarose**

Precise molecular recognition is a hallmark of many natural biological receptors and biocatalysts. A high degree of chemical discrimination is important because receptors and enzymes need to perform biochemical functions only with cognate ligands or substrates from a complex mixture of compounds whose constituents typically include closely related analogs. Likewise, any engineered enzyme or receptor that is used to target cAMP must be endowed with similar

† Funding for this work was provided by NIH (GM59343) and the Yale Diabetes and Endocrinology Research Center (DERC). M.K. was supported by Sankyo Co. LTD of Japan. R.R.B. is the recipient of a Hellman Family Fellowship and a fellowship from the David and Lucile Packard Foundation.

* To whom correspondence should be addressed. E-mail: ronald.breaker@yale.edu. Tel: (203) 432-9389. Fax: (203) 432-5713.

‡ Current address: Sankyo Co., LTD, 2-58, Hiromachi 1-Chome, Shinagawa-Ku, Tokyo 1408710, Japan.

10.1021/bi000149n CCC: $19.00
Published on Web 07/06/2000

discriminatory powers if it is to function stringently in complex chemical mixtures such as those found in cells. Independent SELEX experiments to isolate aptamers for ATP (*11*), nicotinamide adenine dinucleotide (NAD^+) (*23*) and *S*-adenosylmethionine (SAM) (*24*), already have provided a series of structurally related RNAs that bind the three ligands with near equal affinity. Each of these aptamers recognizes the adenosine moiety that is common between the three ligands. Unfortunately, these aptamers do not provide a means by which specific molecular recognition of independent adenosine-containing compounds can be achieved from a complex mixture of molecules.

The tertiary structure analysis of the ligand-binding core of these adenosine-binding aptamers (*25*−*27*) indicates that each aptamer interacts only with the adenosine moiety, whereas the groups appended at the 5′ position of the ligand are exposed to solvent. Since this class of aptamers does not form a structure that could interact differently with various chemical substituents at the 5′ position, it serves as a somewhat promiscuous receptor of compounds adjoined to the 5′ carbon of adenosine. Despite its versatile ligand specificity, this repeatedly isolated aptamer for adenosine does not measurably bind to cAMP-derivatized agarose (Koizumi and Breaker, unpublished data). Therefore, we set out to determine whether new RNA aptamers could be isolated that selectively bind cAMP while precluding the binding of ATP and other adenosine-containing compounds.

MATERIALS AND METHODS

Nucleic Acids. Synthetic DNAs and RNAs were prepared by automated synthesis (Keck Biotechnology Resource Laboratory, Yale University) and were purified by denaturing (8 M urea) polyacrylamide gel electrophoresis (PAGE) followed by crush/soak elution from the gel (*21*). Purine riboside 3′,5′-cyclic monophosphate (cPMP) was synthesized from purine riboside (Aldrich) according to the procedure of Genieser et al. (*28*). The adenosine analogs 8,5′-*O*-cycloadenosine and N^3,5′-cycloadenosine were synthesized according to the procedures of Ikehara et al. (*29*) and Verheyden and Moffatt (*30*), respectively. The radionucleotides [α-^{32}P]UTP and [γ-^{32}P]ATP were purchased from Amersham, and [^{32}P]cAMP was purchased from ICN. All other analogs of cAMP were purchased from Sigma.

In Vitro Selection Protocols. An initial population of RNA transcripts (5′-pppGGAAGAGAUGGCGAC[N_{50}]CGGUAAGCUUGGCAC) was prepared by in vitro transcription using the appropriate synthetic DNA template that carries the T7 RNA polymerase (T7 RNAP) promoter. The initial large-scale transcription reaction, conducted essentially as described previously (*21*), provided ∼10^{14} RNA sequence variants. To remove unincorporated nucleotides and to exchange the buffer mixture, the resulting RNA transcripts were precipitated using ethanol and pelleted by centrifugation. The RNA was resuspended in binding buffer [20 mM Tris-HCl (pH 7.5 at 23 °C), 450 mM NaCl, 100 mM KCl, 10 mM $MgCl_2$, 1 mM $MnCl_2$, and 5 mM $CaCl_2$] and passed through a NICK Spin column (Pharmacia), and the appropriate fractions containing RNA were recovered. Approximately 1 nmol of RNA in 200 μL of binding buffer was incubated at 60 °C for 5 min and allowed to cool at 23 °C for 10 min. The RNA population was incubated with an equal volume of a cAMP−agarose slurry (4% beaded agarose, 3.2 μmol of cAMP/mL of packed gel) in binding buffer for 5 min. The slurry was loaded onto a Micro Bio-Spin Chromatography Column (Bio-Rad). The matrix was subsequently washed with 6 bed volumes (200 μL × 6) of binding buffer, and the RNAs that were selectively retained by the cAMP−agarose resin were recovered by affinity elution with 6 bed volumes of binding buffer containing 4 mM cAMP. The latter fractions were pooled, and the selectively eluted RNA was precipitated with ethanol. The recovered RNAs were amplified by reverse transcription followed by the polymerase chain reaction (RT-PCR) as described previously (*21*) using primer 1 (5′-GTGCCAAGCTTACCG) and primer 2 (5′-GAATTCTAATACGACTCACTATAGGAAGAGATGGCGAC). The resulting double-stranded DNA was used in an in vitro transcription reaction to prepare the RNA population for the subsequent round of selection.

Progress of the elutions at each round of selection was monitored by spotting 4 μL of eluant from each fraction on Whatman chromatographic paper (3MM) and quantitating the dried samples using a PhosphorImager and ImageQuaNT software (Molecular Dynamics). Approximately 45% of the RNA population generated after five rounds of selection (G5) was recovered during the elution with 4 mM cAMP. The subsequent population was cloned using a TOPO-TA cloning kit (Invitrogen) and sequenced using a ThermoSequenase kit (Amersham).

For reselection, a mutagenized DNA template (5′-GTGCCAAGCTTACCGTGCGACAAGTCGTTTTAGTCGCCATCTCTTCCTATAGTGAGTCGTATTAG) was synthesized with a degeneracy (*31*) of 0.21 per position as indicated by the underlined nucleotides. The synthetic DNA was made double stranded by reverse transcriptase-mediated extension using primer 3 (5′-GAATTCTAATACGACTCACTATA), and the resulting templates were transcribed using T7 RNAP (*21*). Approximately 200 pmol representing ∼10^{13} variant RNAs was prepared as described above, and 100 μL of RNA solution in binding buffer was incubated with an equal volume of cAMP−agarose. The bound RNAs were selectively eluted from the matrix as described above and precipitated with ethanol. The recovered RNAs were treated for 1 h with 10 units of alkaline phosphatase (AP; Boehringer Mannheim) according to the manufacturer's directions, and then heated to 95 °C for 1 min to eliminate residual AP activity. The dephosphorylated RNAs were recovered by precipitation with ethanol and incubated for 30 min with 5 U T4 polynucleotide kinase (T4 PNK; New England Biolabs) and [γ-^{32}P]ATP according to the manufacturer's directions. The 5′-labeled RNAs were recovered by precipitation with ethanol, resuspended in 10 μL of deionized H_2O, and subjected to periodate oxidation and β-elimination as described previously (*31*). The latter treatment was used to generate a 3′-terminal phosphate group when necessary (e.g., Figure 4B, structure *ii*). After precipitation of the RNA products with ethanol, the selected molecules were ligated to a chemically synthesized oligoribonucleotide, termed "T7 promoter RNA" (5′-CUAAUACGACUCACUAUA), that encodes the promoter sequence for T7 RNAP. Ligation reactions were conducted at 4 °C for 16 h with T4 RNA ligase (Boehringer Mannheim) using the manufacturer's recommended buffer conditions. Ligation products were amplified by RT-PCR, and the resulting DNA templates were

transcribed by T7 RNAP to prepare the next population of RNAs. The G4 population was cloned and sequenced as described above.

Boundary Analysis Experiments. Individual RNA clones were ^{32}P labeled either at their 5′ terminus with T4 PNK and [γ-^{32}P]ATP or at their 3′ terminus with T4 RNA ligase and [5′-^{32}P]pCp, followed by purification using denaturing 10% PAGE. Purified RNAs (30−50 pmol) were subjected to random cleavage in the presence of 50 mM sodium carbonate (pH 9.0) and 1 mM ethylenediaminetetraacetic acid (EDTA) by heating to 95 °C for 9 min. The resulting nested set of RNAs was combined with 50 μL of cAMP−agarose slurry and incubated at 23 °C for 5 min. The mixture was transferred to a column, and washed with 6 bed volumes of binding buffer followed by 6 bed volumes of binding buffer containing 4 mM cAMP. Samples from these fractions were examined by denaturing 10% PAGE. G-specific cleavage ladders were generated by incubating RNA in 10 μL containing 25 mM sodium citrate (pH 5.0 at 23 °C), 7 M urea, 1 mM EDTA, and RNase T1 (Boehringer Mannheim) for 15 min at 55 °C.

The generation of RNA transcripts with 2′,3′-cyclic phosphate groups was achieved by transcribing a DNA template for T7 RNAP that yields a fusion between the class I aptamer and a hammerhead ribozyme. Unlabeled precursor RNA transcripts or similar internally ^{32}P-labeled RNAs were purified by PAGE. Unlabeled RNAs were dephosphorylated with AP, and then 5′ ^{32}P-labeled using T4 PNK as described above. Internally labeled RNAs were treated with AP to generate a free 5′-hydroxyl group. The resulting RNAs were incubated under permissive reaction conditions for the ribozyme, and the RNA fragments corresponding to aptamers *iii* and *iv* (Figure 4B) that are terminated with 3′,5′-cyclic phosphate were recovered from the gel by crush/soak isolation. The resulting RNAs were used in matrix-binding assays as described in the text.

Equilibrium Filtration Analysis. The dissociation constant (K_D) for the 31-nucleotide cAMP-b RNA was determined by equilibrium filtration analysis (*32*). Various concentrations of 5′-phosphorylated RNA (0.1−30 μM as indicated) were incubated with [^{32}P]cAMP (final concentration 0.025 μM) in 50 μL of binding buffer. The mixture was transferred to a Micron YM-3 Centrifugal Filter Device (Millipore) and spun at 13000*g* at 4 °C for 8 min, producing a filtrate of 12 ± 2 μL. Aliquots (2 μL) from above and below the membrane were spotted onto Whatman paper (3MM), dried, and quantitated by PhosphorImager. The fraction of cAMP bound to RNA was calculated as described previously (*31*).

Assessment of Ligand Specificity. The relative binding affinities of various cAMP analogs were qualitatively determined using a two-step elution protocol. RNA aptamers that were 5′ ^{32}P-labeled using T4 PNK were incubated with 50 μL of cAMP−agarose at 23 °C for 5 min. In the first step, the mixture was transferred to a column and washed with 6 bed volumes of binding buffer followed by 6 bed volumes of buffer containing 0.5 mM of a specific compound as designated for each assay. This pre-elution removed a specific fraction of the total RNA that was originally immobilized. In the second step, the column was eluted with 6 bed volumes of binding buffer containing 4 mM cAMP. The relative binding affinity for each analog was determined by comparing the relative amount of RNA eluted in the first step to the total amount of RNA eluted in both steps. We find that when 6 bed volumes of 0.5 mM cAMP are subsequently applied to the pre-eluted column, an amount of RNA is recovered that is equivalent to that isolated during the pre-elution step. Therefore, 0.5 mM cAMP gives 50% elution of the total amount of RNA eluted during both steps.

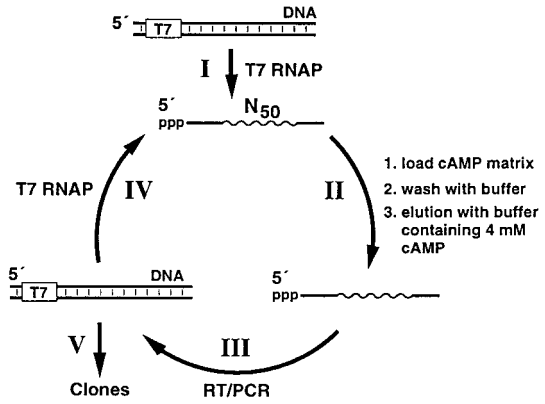

FIGURE 1: In vitro selection of cAMP-specific aptamers from a population of random-sequence RNAs. (**I**) RNA is prepared by in vitro transcription from a mixture of ~6×10^{14} double-stranded DNA templates using T7 RNA polymerase (T7 RNAP). Each template is comprised of a 50-nucleotide domain of random sequence that is flanked by primer-binding sites, one of which includes the promoter for T7 RNAP (T7). (**II**) Purified RNA products are mixed with binding buffer and loaded onto a column packed with an agarose affinity matrix that is derivatized with cAMP. Unbound RNAs are removed by washing the matrix with binding buffer. RNAs that are selectively bound to the matrix via interactions with immobilized cAMP are specifically recovered by elution with binding buffer containing 4 mM cAMP. (**III**) Recovered RNAs are amplified by reverse transcription followed by the polymerase chain reaction (RT/PCR). (**IV**) The resulting double-stranded DNAs are transcribed to generate the subsequent population of RNA. (**V**) Double-stranded DNA from the final round of selection is cloned for further analysis.

RESULTS AND DISCUSSION

Isolation of cAMP-Specific Aptamers. RNA aptamers for cAMP were isolated by in vitro selection from a population of 80-nucleotide RNA transcripts, each containing a 50-nucleotide region of random sequence (Figure 1). After four rounds of selective amplification (G4), more than 20% of the RNA population binds to the cAMP-derivatized column matrix in binding buffer (see Materials and Methods for details) and is subsequently eluted with binding buffer containing 4 mM cAMP. Likewise, approximately 45% of G5 RNA is selectively eluted by addition of free cAMP. This fraction of RNA did not significantly increase with further rounds of selection.

To test whether G5 RNA can discriminate between cAMP and 5′-phosphorylated derivatives of adenosine such as ATP, the population was loaded onto a column containing an agarose matrix that was derivatized with 5′-AMP. The class of ATP-binding aptamers described by Sassanfar and Szostak (*11*) readily binds to this matrix (*32*). In contrast, we observed that the G5 RNA population does not bind the 5′-AMP-derivatized matrix (data not shown), indicating that novel types of aptamers had been enriched by the selection process.

The G6 population was cloned, and the plasmid DNA from nine colonies was sequenced. Four individuals with significantly different nucleotide sequences were identified (Figure

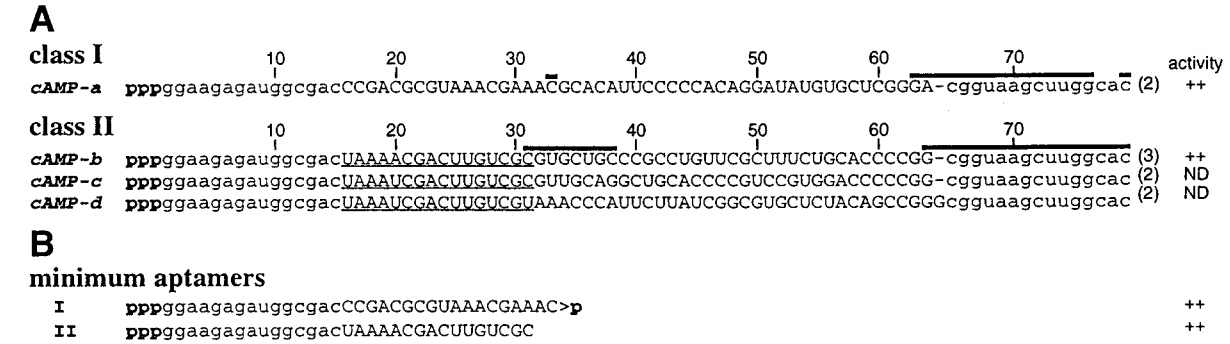

FIGURE 2: Nucleotide sequences of four cAMP aptamers isolated by in vitro selection. (A) The sequences of the primer-binding sites were held constant during the selection process and are depicted with lower case letters, where **p** represents phosphate. The 16-nt domain that is conserved in class II RNAs is underlined. Overlines identify the 3′-terminal nucleotides of various truncated RNAs that retain full cAMP−agarose binding function. For example, the cAMP-a RNA that terminates at C33 binds cAMP−agarose, while the *n+1* RNA construct that terminates with G34 is inactive. Numbers in parentheses reflect multiple clones. The percent of RNA that is retained by the cAMP affinity matrix and is subsequently eluted by free cAMP, which reflects the efficiency of aptamer function, is represented by +++ (>60%), ++ (40−60%), + (20−40%), − (<20%), or ND (not determined). Values reflect the total amount of RNA loaded on the matrix. (B) The minimized RNAs for class I and class II aptamers are 33 and 31 nucleotides in length, respectively. The 5′-terminal phosphate group of both RNAs is required for maximum binding function. In addition, a 2′,3′-cyclic phosphate group is necessary for binding activity of the truncated class I aptamer.

2). Three of these individuals (cAMP-b, cAMP-c, and cAMP-d) were categorized as "class II" aptamers by the presence of a nearly-identical 16-nt sequence located immediately adjacent to the 5′ primer-binding site. The remaining sequence (cAMP-a) does not carry this same conserved sequence element. The cAMP-a RNA was categorized as a "class I" aptamer.

Minimal Ligand-Binding Domains. The minimum sequence requirements for the two classes of aptamers were determined by boundary analysis experiments. RNAs representing class I or class II aptamers each were radiolabeled with ^{32}P either at their 5′ or at their 3′ termini and subjected to partial alkaline-mediated chain cleavage. The resulting nested set of RNAs was delivered to a column packed with cAMP−agarose. Truncated RNAs that no longer bind cAMP pass through the column, while RNAs that bind cAMP are retained by the matrix.

PAGE analysis of the distribution of RNAs derived from 5′ ^{32}P-labeled cAMP-a transcripts (Figure 3) was used to establish the shortest class I RNA that binds cAMP and to establish the importance of flanking sequences on the function of the minimal RNA aptamer. In this case, the RNA aptamer can be truncated to nucleotide position C33 with full retention of cAMP-binding function. However, many longer RNAs that include the minimum active domain do not bind the cAMP−agarose matrix, suggesting that secondary or tertiary structures formed using the nucleotides 3′ of the minimum aptamer domain can modulate ligand binding. Likewise, an analysis conducted with 3′ ^{32}P-labeled cAMP-a RNA reveals that the 5′-terminal guanosine residue (G1) is essential for aptamer function (data not shown). As a result, we conclude that the smallest contiguous class I aptamer based on cAMP-a is 33 nucleotides in length (Figure 2B).

The class II aptamer cAMP-b was examined using a similar boundary analysis study, which reveals a minimal contiguous domain of 31 nucleotides (Figure 2B; data not shown). For both class I and class II motifs, the 5′ primer-binding sites of the original RNA pool have become integral components of the aptamer structure.

Secondary Structure Models. RNA secondary structure predictions for the two classes of aptamers were made using the Zuker RNA *mfold* computer algorithm (*33*). The minimized class I aptamer is predicted to form a dumbbell-like structure (Figure 4A), in which the 10 nucleotides at the 5′ end of the RNA remain unpaired. To test the structural models for class I and class II aptamers, we examined the patterns of spontaneous RNA cleavage both in the absence and in the presence of cAMP. A similar strategy has been used to examine the secondary and tertiary structure features of other aptamers using the protocol described previously (*34*). When incubated in binding buffer without cAMP, both aptamers have cleavage patterns that are consistent with the structural models predicted by the Zuker algorithm that are depicted in Figure 4A,C. Specifically, spontaneous strand scission is reduced in regions that are predicted to reside in base-paired structures, while unpaired regions cleave significantly faster (data not shown). When cAMP is added, the cleavage pattern is altered at ∼18 positions in a fashion that is consistent with 'adaptive binding' of the ligand. In other words, ligand binding brings about an ordered structuring of the otherwise unstructured bulges and loops of each aptamer.

Interestingly, a chemically synthesized 5′ ^{32}P-labeled RNA encompassing the 33 nucleotides of the minimal class I aptamer is incapable of binding the cAMP-agarose matrix (Figure 4B, structure *i*). This synthetic RNA is identical to the minimal functional RNA identified in the boundary analysis experiments described above (Figure 3), with the exception that the 2′,3′-cyclic phosphate that is generated by alkaline-mediated RNA cleavage is absent. To examine the importance of the phosphate moiety at the 3′-terminus, a 34-nucleotide RNA containing an additional G residue compared to the minimal cAMP-a RNA was prepared by chemical synthesis. This RNA was incapable of binding to the cAMP−agarose matrix, just as predicted by the original boundary analysis (data not shown). Interestingly, conversion of the 34-nucleotide RNA into a 33-nucleotide RNA with a 3′-terminal phosphate moiety (Figure 4B, structure *ii*), via periodate-mediated oxidation and β-elimination of the 3′ nucleoside (*35*), yielded an RNA product that also failed to bind the cAMP−agarose matrix.

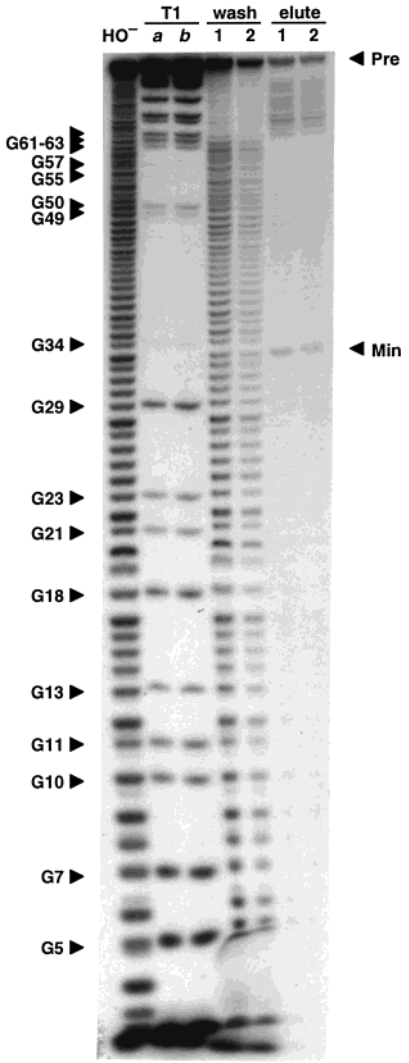

FIGURE 3: Boundary analysis experiment for determining the 3′ terminus of the functional domain of the class I cAMP aptamer. RNAs representing a single full-length cAMP-a clone were 5′ ^{32}P-labeled and subjected to partial alkaline-mediated degradation to produce a nested set of truncated RNAs. The resulting degradation products were loaded on to a chromatographic column packed with cAMP agarose, which selectively complexes with truncated RNAs that retain cAMP-binding function. Unbound RNAs were collected in the wash, and bound RNAs were eluted with 4 mM cAMP. Aliquots of the samples were examined by PAGE and imaged by autoradiography. Ribonuclease T1 treatment of the RNA (T1) generates RNA products that are cleaved on the 3′ side of G residues. The notations *a* and *b* represent the use of 0.025 and 0.05 units/μL of RNase T1, respectively. Bands representing products of alkaline-mediated RNA cleavage on the 3′ side of each base are indicated on the left. The full-length RNA precursor (Pre) and the minimal RNA that retains cAMP-binding function (Min) are identified accordingly.

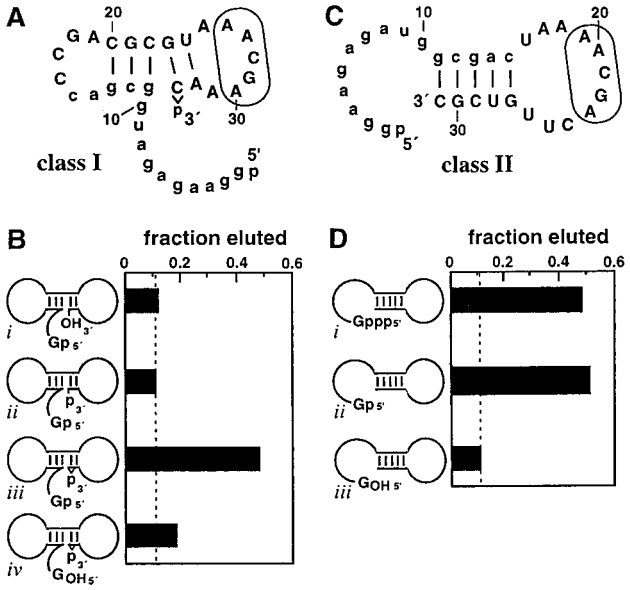

FIGURE 4: Minimum class I and class II cAMP aptamers. (A) Sequence and secondary structure model for a representative class I aptamer based on the minimized cAMP-a clone. The 3′-terminal phosphate group is represented in a 2′,3′-cyclic phosphate configuration. (B) Binding of class I aptamers to cAMP−agarose is dependent on the chemical structure of the 5′ and 3′ termini. The fraction of the total RNA that is delivered to a cAMP−agarose column that is specifically eluted with 4 mM cAMP is plotted for different constructs based on the 33-nucleotide domain of cAMP-a. The dashed line reflects the level of nonspecific binding under the assay conditions used. (C) Sequence and secondary structure model for a representative class II aptamer based on the minimized cAMP-b clone. (D) Binding of class II aptamers to cAMP−agarose is dependent on the chemical structure of the 5′ terminus. The fraction of the total RNA that is delivered to a cAMP−agarose column that is specifically eluted with 4 mM cAMP is plotted for different constructs based on the 31-nucleotide domain of cAMP-b. Note that nucleotides 1−15 (lowercase) in each of the two aptamers are derived from the 5′ primer binding sequence. Both classes share the sequence 5′-AACGA in the hairpin loop (encircled).

We speculated that perhaps the aptamer requires the 2′,3′-cyclic phosphate group that is generated by alkaline-mediated cleavage, and that this requirement is not necessary in the context of the full-length RNA clone. To further examine the importance of the 5′ and 3′ termini, we generated two RNA constructs that retain the 2′,3′-cyclic phosphate group and in addition have either a 5′-phosphate or a free 5′-hydroxyl terminus (Figure 4B, structures *iii* and *iv*, respectively). Generation of RNAs carrying the 2′,3′-cyclic phosphate group was achieved by appending them to the hammerhead ribozyme, such that ribozyme cleavage produced the desired cyclic phosphate product (see Materials and Methods). Only those RNAs containing both the 5′-phosphate and the 2′,3′-cyclic phosphate termini show maximal binding to the agarose matrix, indicating that phosphate groups at both ends and in the proper configuration are essential for ligand-binding function.

Similarly, the minimum class II aptamer formed by a 31-nucleotide RNA is predicted by the RNA *mfold* program to form a 5 base-pair helix that is flanked by a 10-nucleotide single-stranded domain and an 11-nucleotide hairpin loop (Figure 4C). This structure has features that are similar to those of the class I structure. For example, the same unpaired nucleotides of the 5′ portion of class I are also unpaired in the secondary structure predicted for class II. In addition, the hairpin loops of the two RNAs each contain an identical six-nucleotide domain (class I: nucleotides 25−30; class II: nucleotides 18−23). These similarities suggest that the two classes of aptamers may form related ligand-binding pockets, despite the differences in their secondary structures.

Unlike its class I counterpart, ligand binding by the 31-nucleotide class II aptamer has no requirement for a 3′-terminal phosphate (Figure 4D, structures *i* and *ii*). However, the aptamer has an absolute requirement for one or more phosphate groups located at the 5′ terminus. For

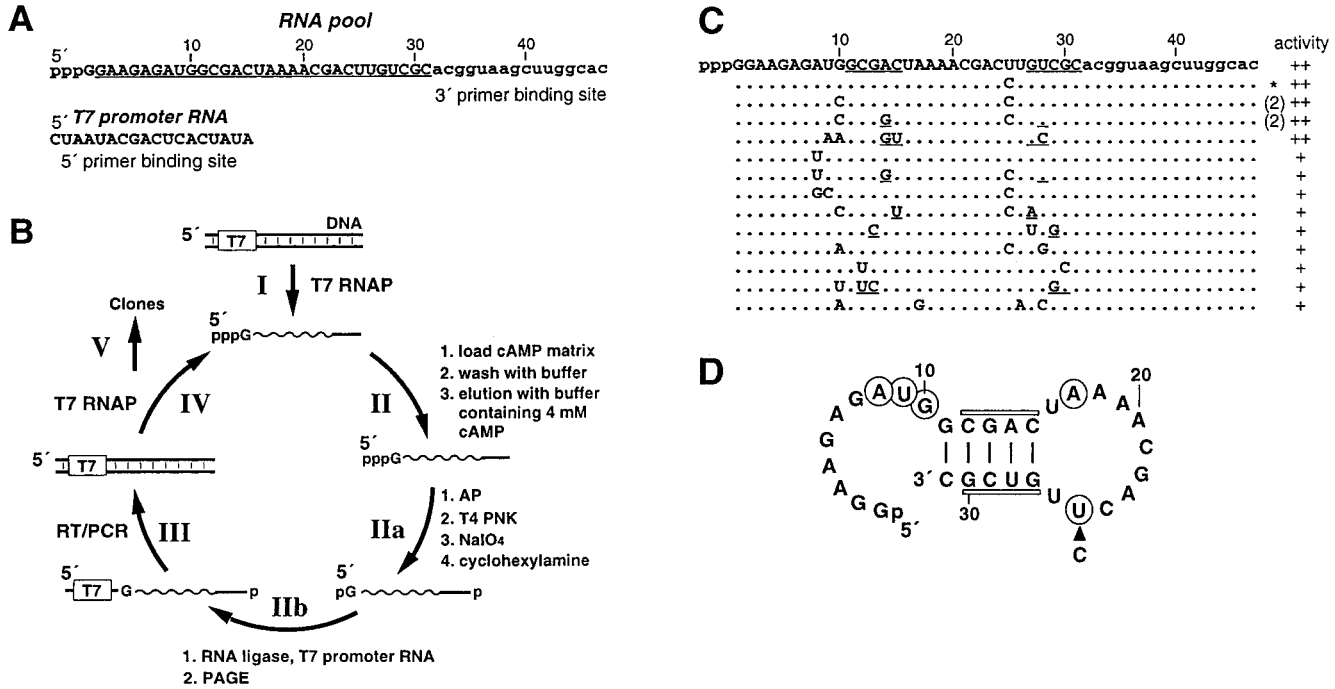

FIGURE 5: Reselection of a minimized class II aptamer. (A) Construct used for the reselection of class II cAMP aptamers. Underlined sequences were mutagenized with a degeneracy (*d*) of 0.21. The first nucleotide was not mutagenized because of the preference that T7 RNAP exhibits for transcripts that begin with guanosine residues. (B) Selection scheme for the isolation of variant class II aptamers from a mutagenized precursor. Steps **I**−**V** are identical to steps **I**−**V** described in Figure 1. However, two additional steps have been added to facilitate amplification. (**IIa**) RNAs that are eluted from the affinity matrix with cAMP are treated with alkaline phosphatase to remove the 5′-triphosphate moiety. A single phosphate group is restored to the 5′ terminus with T4 polynucleotide kinase (T4 PNK). In addition, a 3′-phosphate terminus is generated by removal of the 3′ nucleoside by periodate-mediated oxidation and β-elimination (*35*). (**IIb**) The resulting RNAs are combined with a 17-nucleotide RNA that encodes the T7 RNA polymerase promoter sequence, and the 2 RNAs are joined using RNA ligase. The ligation products are purified by PAGE prior to amplification by RT/PCR. (C) Artificial phylogeny of functional class II aptamers isolated by reselection. Nucleotides that differ from the parent cAMP-b sequence (top) are identified, while dots represent unchanged nucleotides. Underlined positions identify base complementary when mutations have occurred that are consistent with the presence of a stem structure. Quantitation of binding activity for each variant is described in the legend to Figure 2. The clone identified with the asterisk carries an additional U residue between nucleotides A6 and G7. Numbers in parentheses reflect multiple clones. (D) Location of tolerated sequence variation in the secondary structure of class II aptamers. Encircled nucleotides tolerate mutations, with only U at position 25 exclusively mutating to C. Open bars identify putative base-paired nucleotides that are supported by apparent covariation.

example, minimized cAMP-b RNA cannot bind to the cAMP−agarose matrix when a free 5′-hydroxyl group is present (Figure 4D, structure *iii*). However, 31-nucleotide RNAs that carry a single 5′-phosphate group added by the action of T4 polynucleotide kinase, or RNAs that carry a triphosphate moiety as a result of T7 RNAP transcription initiation with GTP, exhibit normal binding to the matrix.

Characterization of the Class II Structural Model. We chose to examine the secondary structure model for class II aptamers due to its dominant representation in the original population of selected RNAs. To investigate the importance of various sequence and structural components of the motif, we subjected a representative RNA aptamer (cAMP-b) to mutagenesis and reselection for cAMP binding. To produce a truncated RNA pool for reselection (Figure 5A), the original RNA sequence located 3′ relative to the aptamer had to be replaced due to its inhibitory characteristics. Therefore, a new truncated construct was designed that contained the minimal 31-nucleotide aptamer appended at its 3′ terminus to a new 16-nucleotide RNA that serves as a primer-binding site for amplification purposes. Unlike much of the original 3′ domain of the cAMP-b clone, this new primer-binding sequence is fully compatible with the ligand-binding function of the adjoining aptamer domain.

In addition, the 5′ primer-binding site of the RNA pool used in the original selection is a significant structural component of both class I and class II aptamers. To probe the importance of the entire cAMP binding domain by reselection, nearly all of this original primer-binding site was subjected to random mutagenesis along with the rest of the 31-nucleotide aptamer domain. As a result, it was necessary to include a new 5′ primer domain in the construct in order to facilitate RT-PCR amplification. Unfortunately, we observed that the addition of even a single G nucleotide to the 5′ end of the minimal cAMP-b RNA causes inactivation of the construct's cAMP-binding activity (data not shown). Therefore, we synthesized a separate 18-nucleotide RNA that carries the promoter sequence for T7 RNA polymerase, which was joined to selected individuals of the RNA aptamer pool after each round of cAMP-mediated elution from the agarose affinity matrix.

A revised selection scheme (Figure 5B) was employed for the reselection of class II aptamers. In contrast to the original aptamer selection (Figure 1), this revised protocol includes two additional stages (IIa and IIb) that involve treatments necessary for attachment of the T7 promoter RNA oligonucleotide. After five rounds of reselection, greater than 40% of the RNA population both bound to the cAMP−agarose affinity matrix and was specifically eluted with cAMP. This population was cloned, and 20 individuals were subjected to nucleotide sequencing. A total of 18 individuals have unique sequence variations compared to the parent cAMP-b

sequence, and 13 of these exhibit affinity to the cAMP affinity matrix.

Comparative sequence analysis of the 13 active variants reveals several important sequence and structural features of the class II motif (Figure 5C). First, the five base pair helix that is predicted by the RNA folding program is supported by numerous nucleotide covariations within many clones (Figure 5D). In most instances, nucleotide changes in the putative helix domain occur in a pattern that retains base complementarity. Second, nucleotides near the 5′ end of the RNA are highly conserved, suggesting that much of the original 5′ primer-binding site is critical for complex formation. Interestingly, the strictly conserved nucleotides 1−6 (pGGAAGA) are also present in the adenosine-binding aptamer isolated previously (*11*, *23*, *24*), where they are known to form direct contacts with the bound ligand (*25*−*27*). However, the exact role of this sequence element in these aptamers remains unclear. Third, the hairpin loop also is highly conserved, indicating that the sequence element that is shared between classes I and II most likely is an important determinant of cAMP binding. In summary, the distribution and identities of the nucleotide changes observed in the cAMP-b variants (Figure 5D) are consistent with the structural model for class II aptamers depicted in Figure 4C.

Functional Characteristics of a Class II Aptamer. The binding buffer used for in vitro selection included several different monovalent and divalent metal ions. We independently examined the importance of each of these components of the selection buffer by conducting binding assays wherein individual metal ions were withheld from otherwise complete buffer mixtures. The 31-nucleotide cAMP-b RNA retains near full binding activity when either the monovalent metal ions Na^+ and K^+ or the divalent metal ions Mg^{2+} and Ca^{2+} are independently withheld from the binding buffer (Figure 6A). However, the absence of all divalent metal ions results in a substantial loss of cAMP binding. In contrast, the presence of low concentrations of Mn^{2+} provides maximum binding activity. Although the binding buffer conditions used for in vitro selection support the maximum observed binding activity, K^+, Mg^{2+}, and Ca^{2+} are unnecessary.

The K_D of the truncated cAMP-b RNA for its corresponding ligand in solution was determined by equilibrium filtration assays (*36*). Different concentrations of 31-nucleotide cAMP-b RNA were combined with a trace amount of ^{32}P-labeled cAMP, and the mixture was subjected to filtration such that the bound versus free cAMP could be quantitated. Under in vitro selection conditions, more than half of the ^{32}P-labeled cAMP becomes bound to RNA when the RNA concentration surpasses 10 μM, thus reflecting the K_D for the aptamer−ligand complex (Figure 6B). Therefore, this individual aptamer recognizes cAMP both free in solution and as a conjugate to the agarose matrix. In comparison, a 21-nucleotide RNA comprising nucleotides 11−31 of cAMP-b does not exhibit cAMP binding, consistent with previous data indicating that the entire 31-nucleotide RNA is needed for cAMP binding. The K_D for cAMP of 10 μM exhibited by class II aptamers is similar to the binding affinities that have been previously established for aptamers that bind small organic compounds (*15*, *16*).

Molecular Recognition Determinants for Class II Aptamers. A series of cAMP analogs was used to examine the binding specificity of the 31-nucleotide cAMP-b RNA. To determine binding specificity qualitatively, a two-step elution assay (*36*) was used wherein the fraction of ^{32}P-labeled RNA that is eluted from a cAMP−agarose column upon addition of the ligand reflects the relative binding affinity. In the first step, the column is pre-eluted with buffer containing 0.5 mM of the test ligand. In the second step, 4 mM cAMP is present in the buffer. For example, the inclusion of 0.5 mM cAMP in the buffer for the first elution yields approximately 50% of the total RNA recovered by both the pre-elution and the elution steps. Since the fraction of total RNA eluted in the first step is dependent on the binding affinity of the free ligand, this protocol makes possible the rapid assessment of binding affinity of various analogs relative to cAMP.

We find that 5′-AMP and ATP are not bound by the truncated cAMP-b RNA, as determined by the observation that no RNA is eluted from the cAMP−agarose matrix by these compounds (Figure 7A). This suggests again that class II cAMP aptamers have distinct molecular recognition capabilities compared to the class of adenosine-binding aptamers isolated previously (*11*, *23*, *24*). However, we also observe that cAMP-b RNA binds adenosine and adenine with

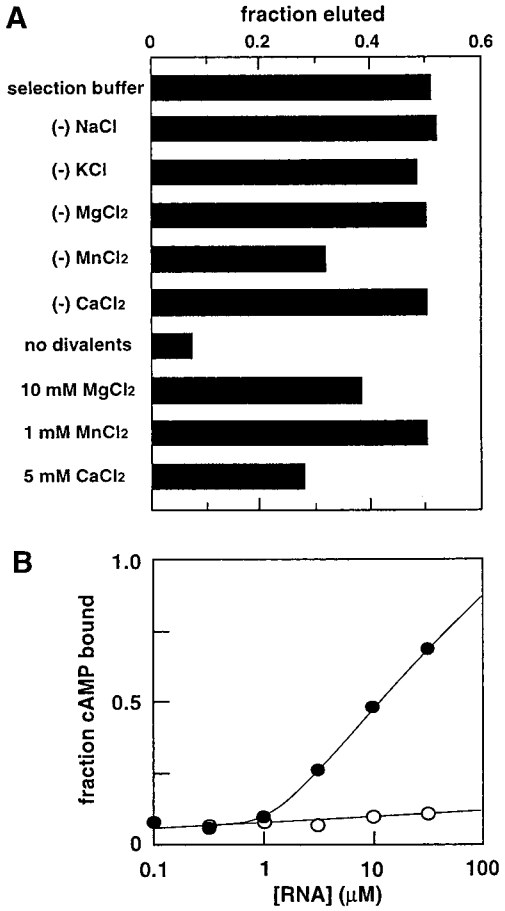

FIGURE 6: Characterization of the class II aptamer. (A) The importance of monovalent and divalent metal cations was assessed by binding and elution assays. The fraction of 31-nucleotide cAMP-b RNA (5′ ^{32}P-labeled) that bound to cAMP−agarose and was subsequently eluted using 4 mM cAMP is plotted for various buffer conditions. (B) Determination of the K_D for the aptamer−ligand complex using equilibrium filtration (*36*). The fraction of total cAMP (^{32}P-labeled) bound to either the 31-nucleotide cAMP-b RNA (filled circles) or a 21-nucleotide aptamer fragment (open circles) is plotted for different RNA concentrations. The concentration of RNA at which the fraction of cAMP bound equals 0.5 reflects the K_D for the aptamer−cAMP complex (10 μM).

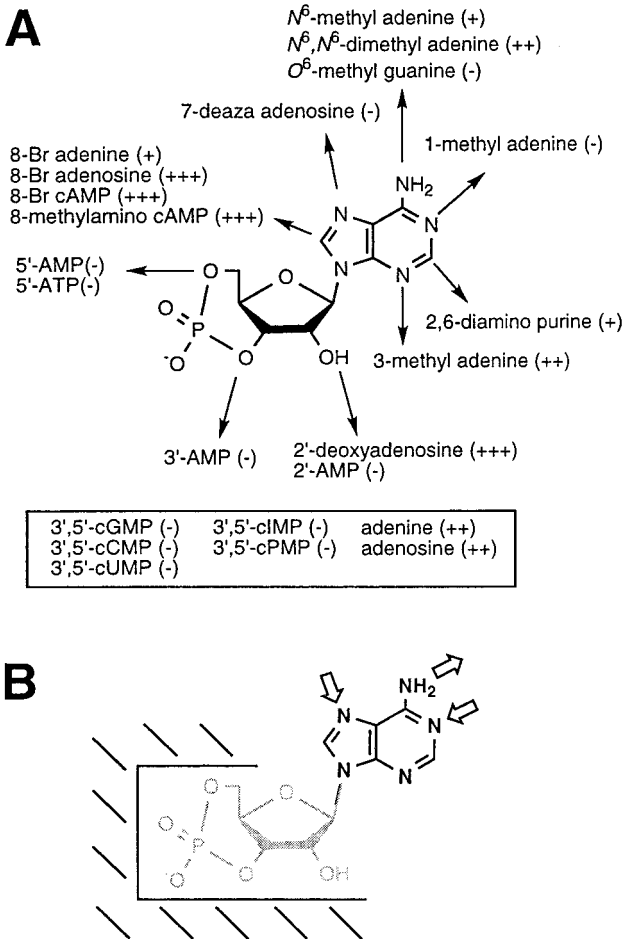

FIGURE 7: Chemical determinants of ligand recognition by class II aptamers. (A) The activities of various cAMP analogs were examined for their ability to elute the 31-nucleotide cAMP-b RNA (5′ ^{32}P-labeled) from a cAMP−agarose matrix. The extent of elution is indicated by (+) and (−) symbols and represents percent of RNA eluted from the column by various cAMP analogs as defined in the legend to Figure 2. 3′,5′-cIMP and 3′,5′-cPMP carry hypoxanthine and purine bases, respectively, in place of the adenine base of cAMP. (B) Summary of the determinants of cAMP recognition by a class II aptamer. Solid lines represent the adenine base that is involved in hydrogen bonding (arrows) and possibly hydrophobic interactions with the aptamer. Directionalities of arrows define each group as a hydrogen bond acceptor (facing toward) or hydrogen bond donor (facing away). The hatched areas represent the pocket formed by the aptamer to accommodate the ribose and cyclic phosphate moieties. This pocket precludes the binding of even closely related analogs of cAMP that have molecular shapes that cannot fit within the footprint of the original ligand.

affinities that are similar to that observed for cAMP. Therefore, the ribose and cyclic phosphate moieties are not essential determinants of the ligand-binding process. However, when the ribose and phosphate moieties are present in the ligand, their composition is critical for ligand−aptamer interaction (see below for further discussion).

Comparison of the binding characteristics of other analogs reveals three positions on the adenine base (N1, N7, and the exocyclic amine at position 6) that might be involved in hydrogen bond formation. Blockage of the N1 position, as found with the analog 1-methyladenine, is consistent with a hydrogen bond donor role for this position. Similarly, replacement of the N7 with carbon as in the analog 7-deazaadenosine also prevents hydrogen bonding at this position. The role of the exocyclic amine at position 6 is more cryptic. N^6,N^6-Dimethyladenine has both hydrogens of the amine replaced by methyl groups, yet the analog is bound by the aptamer apparently without loss of affinity. However, purine riboside 3′,5′-cyclic monophosphate (3′,5′-cPMP) cannot elute the RNA from the affinity matrix to any measurable extent. This suggests that the exocyclic amine at position 6, which is missing in 3′,5′-cPMP, is a critical determinant of ligand binding. It is possible that the exocyclic amine serves as a hydrogen bond donor, but the loss of this contact due to methylation might be offset by the increase in hydrophobic character of the base moiety, which may increase ligand affinity by improvement of base stacking potential. It has been established that N^6,N^6-dimethyladenine is more hydrophobic than N^6-methyladenine (*37*), which is consistent with this hypothesis.

Additional features of the ligand-binding character of the aptamer are revealed by the performance of other analogs. The observation that 2′-deoxyadenosine binds with greater affinity that does cAMP is difficult to rationalize considering the fact that the ribose group can be eliminated without dramatic gain or loss of affinity. The improved affinity resulting from this change could be explained by the alleviation of a steric clash near the 2′ carbon, or it could also be explained by the increase in hydrophobic character of the ligand that may favor tighter binding. Finally, analogs that carry modifications at the C8 position bind with the highest affinity, which indicates that the aptamer may favor cAMP derivatives that more closely match the chemical structure of cAMP when coupled to the agarose matrix.

A summary of the chemical groups that are important for ligand recognition is provided by Figure 7B. Presumably, the adenine base is directly recognized by the aptamer by hydrogen bonding with positions N1, N7, and the exocyclic amine at position 6. Additional affinity for the ligand might be derived through hydrophobic interactions, perhaps through base stacking. In contrast, the ribose and cyclic phosphate moieties appear not to be involved in direct molecular contacts with the aptamer. However, increasing the size or flexibility of the groups at the 2′, 3′, and 5′ positions all result in loss of binding.

These findings indicate that the aptamer forms a structure that is a nearly-perfect match for the size and shape of the ribose and phosphate moieties of cAMP. Even subtle alteration of this structure such as hydrolysis of the phosphodiester ring results in steric exclusion of the ligand. Moreover, the patterns of molecular recognition determinants of class II aptamers are distinct from those of previously isolated adenosine and ATP aptamers. For example, the class II aptamer apparently forms hydrogen bonds only with adenine at positions N1, N7, and the exocyclic amine at position 6. In contrast, the ATP aptamer previously isolated (*11*) contacts the adenine only at position N1 and the exocyclic amine at position 6 of adenine, while apparently also forming a productive contact with the ligand's 2′-hydroxyl group. This is consistent with the conclusion that the cAMP-binding aptamers identified in this study use different adenine-binding structures.

Examining the Glycosidic Bond Conformation Required for Ligand Binding. The glycosidic bond of nucleosides and nucleotides can adopt two conformations, anti and syn (Figure 8A) (*38*). Single-crystal X-ray analysis of cAMP has shown both conformations of cAMP per asymmetric unit

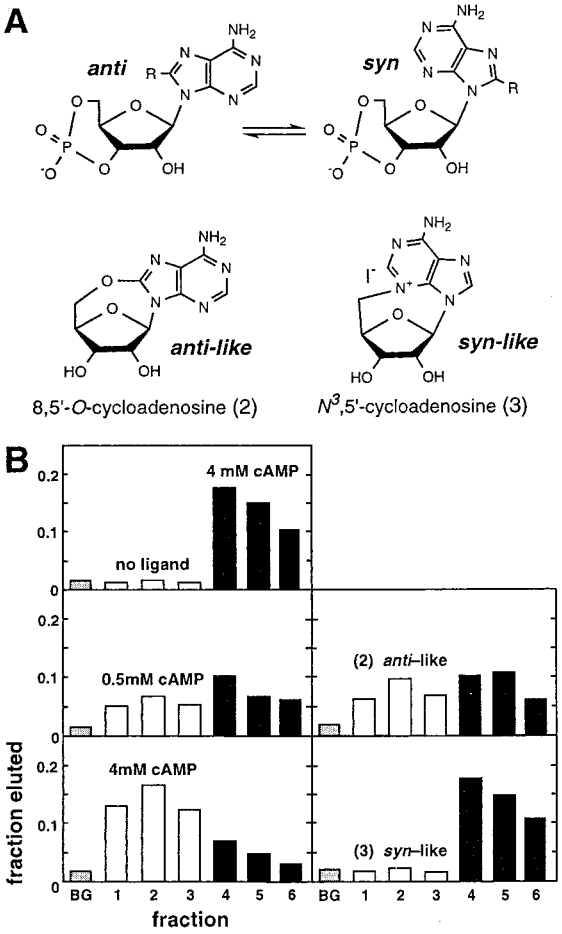

FIGURE 8: Importance of the glycosidic bond conformation for ligand binding. (A) the syn-anti equilibrium of cAMP (R = H) is shifted toward syn when bulky groups are present at the C8 position (e.g., R = Br, Cl, methylamino, etc.) (*40*, *41*). The two adenosine derivatives 8,5′-*O*-cycloadenosine (**2**) and N^3,5′-cycloadenosine (**3**), respectively, form the anti-like and syn-like conformational isomers that are found with adenosine and cAMP. (B) Elution profiles of the 31-nucleotide cAMP-b RNA bound to cAMP−agarose using cAMP and compounds **2** and **3**. Shaded bars reflecting the background level of RNA elution in the absence of any ligand are labeled BG. Open and filled bars reflect the fraction of RNA eluted with the designated ligand or with a 4 mM cAMP wash, respectively. Elution experiments were conducted as described for the data presented in Figure 7A, where each bar includes 2 bed volumes of eluant.

(*39*). These two conformational variants of cAMP carry the ribose and phosphate moieties in very different spatial locations. Although the adenine moiety alone is sufficient for ligand binding by cAMP-b RNA, we speculated that either the anti or the syn conformation of cAMP might be selectively bound while its opposite conformer might be entirely excluded. This speculation was based on the fact that the ribose and phosphate moieties of cAMP appear to precisely fit in a pocket formed by the aptamer that excludes analogs with subtle changes in the size or shape of these groups.

To investigate whether the aptamer exhibits a preference for ligand conformation, we synthesized and tested two nucleoside analogs, 8,5′-*O*-cycloadenosine (**2**) and N^3,5′-cycloadenosine (**3**), which simulate the anti and syn conformations of adenosine, respectively (Figure 8A). Analysis of the relative binding affinities of these analogs using the two-step elution procedure (Figure 8B) reveals that 4 mM 8,5′-*O*-cycloadenosine facilitates elution of cAMP−agarose-immobilized RNA aptamer with an efficiency near that of cAMP. In contrast, 4 mM N^3,5′-cycloadenosine has no observable ability to elute RNA from the matrix. These findings are consistent with the view that class II cAMP aptamers specifically recognize cAMP in its anti conformation.

It is interesting to note that the adenosine and cAMP analogs that are modified at the 8 position all are more tightly bound to the aptamer than is the original target ligand. This can be rationalized by the fact that the aptamer has been selected to bind cAMP that is tethered to agarose via a linker to the C8. However, it is known that the glycosidic bond in nucleosides and nucleotides with C8 substitutions favor the syn conformation. (*40*, *41*) Since the two conformers are in an equilibrium state, we speculate that the aptamer might bind and trap the ligand in its anti conformation. A precedent for this effect is provided by crystallographic data of the complex between liver alcohol dehydrogenase and 8-bromoadenosine analogs of NAD^+. The protein binds the analogs in their anti conformation despite the fact that free 8-bromoadenosine favors the syn conformation (42).

CONCLUSIONS

The class II cAMP aptamer examined in this study exhibits precise discrimination between cAMP and its analogs 5′- and 3′-AMP, which differ only by the hydrolyzed cyclic phosphodiester moiety. In contrast, fragments of cAMP such as the nucleoside moiety (adenosine) and the base moiety (adenine) are also recognized by the aptamer with nearly-equal affinity. Presumably, the ribose and cyclic phosphate moieties of cAMP are not directly involved in the molecular recognition process, but they maintain a size and shape that is compatible with the tertiary structure of the aptamer. Moreover, the aptamer must create a pocket to accommodate these two extraneous moieties. Even subtle alterations (phosphodiester ring hydrolysis) prevent ligand binding, most likely due to steric clashes between ligand and RNA. There is no evidence that this cavity forms discrete productive interactions with the ribose or the phosphate groups.

A number of RNA and DNA aptamers isolated previously also exhibit high affinity and exquisite selectivity for their corresponding ligands (*3*−*5*). In this case, the cAMP-b RNA presumably employs a combination of hydrogen bonding and hydrophobic interactions to specifically recognize only a portion of the cAMP ligand. In addition, the RNA exploits steric interactions to preclude the binding of certain derivatives of the target ligand. These modes of molecular recognition establish a pattern of ligand contacts that precludes the binding of the syn form of cAMP despite the fact that only the adenosine portion of the compound is directly bound by the aptamer.

The integration of aptamers into mRNAs has recently proven to be an effective way to introduce ligand-dependent control over gene expression in living cells (*43*). In addition, RNA aptamers have been used as allosteric binding sites for engineered ribozymes that are specifically controlled by small effector molecules (*21*, *22*, *34*−*46*). Class II aptamers do retain cAMP-binding function under conditions that approach those found in living cells (Figure 6). However, it appears that both classes of aptamers isolated in this study might

not be conducive to insertion into the interior of larger RNAs, as both the 5′ and 3′ termini of the RNAs have special structural and chemical characteristics that would most likely be disrupted. Perhaps these aptamers would be best suited for integration at the 5′ end of engineered RNAs so that the structural requirements for ligand binding would not be adversely affected.

The putative structural pocket that accommodates the ribose and cyclic phosphate moieties in class II aptamers apparently envelops all available faces of this part of the ligand. Complete concealment of the cyclic phosphate group within this pocket could preclude access by other reactive groups that could react with cAMP. If true, then this aptamer would not provide a good preformed substrate-binding site for further development of cAMP utilizing enzymes. However, the close proximity of RNA to the ribose and phosphate moieties leaves open the possibility that mutations might result in the formation of direct contacts with the ribose and phosphate groups. Such contacts are necessary to form an active site that facilitates chemical catalysis with cAMP as a substrate. Therefore, the cAMP-specific aptamers described herein and elsewhere (*46*) are potential starting points for the engineering of novel cAMP-utilizing ribozymes.

REFERENCES

1. Houslay, M. D., and Milligan, G. (1997) *Trends Biochem. Sci. 22*, 217−224.
2. Perry, M. J., and Higgs, G. A. (1998) *Curr. Opin. Chem. Biol. 2*, 472−481.
3. Gold, L., Polisky, B., Uhlenbeck, O., and Yarus, M. (1995) *Annu. Rev. Biochem. 64*, 763−797.
4. Osborne, S. E., and Ellington, A. D. (1997) *Chem. Rev. 97*, 349−370.
5. Famulok, M. (1999) *Curr. Opin. Chem. Biol. 9*, 324−329.
6. Ellington, A. D., and Szostak, J. W. (1990) *Nature 346*, 818−822.
7. Ellington, A. D., and Szostak, J. W. (1992) *Nature 355*, 850−852.
8. Famulok, M., and Szostak, J. W. (1992) *J. Am. Chem. Soc. 114*, 3990−3991.
9. Connell, G. J., Illangesekare, M., and Yarus, M. (1993) *Biochemistry 32*, 5497−5502.
10. Majerfeld, I., and Yarus, M. (1994) *Nat. Struct. Biol. 1*, 287−292.
11. Sassanfar, M., and Szostak, J. W. (1993) *Nature 364*, 550−553.
12. Huizenga, D. E., and Szostak, J. W. (1995) *Biochemistry 34*, 656−665.
13. Wang, Y., and Rando, R. R. (1995) *Chem. Biol. 2*, 281−290.
14. Lato, S. M., Boles, A. R., and Ellington, A. D. (1995) *Chem. Biol. 2*, 291−303.
15. Wallis, M. G., von Ahsen, U., Famulok, M., and Schroeder, S. (1995) *Chem. Biol. 2*, 543−552.
16. Wallis, M. G., Streicher, B., Wank, H., von Ahsen, U., Clodi, E., Wallace, S. T., Famulok, M., and Schroeder, S. (1997) *Chem. Biol. 4*, 357−366.
17. Wallace, S. T., and Schroeder, R. (1998) *RNA 4*, 112−123.
18. Breaker, R. R. (1997) *Chem. Rev. 97*, 371−390.
19. Pan, T. (1997) *Curr. Opin. Chem. Biol. 1*, 17−25.
20. Breaker, R. R. (1999) in *Intracellular Ribozyme Applications: Principles and Protocols*, Horizon Scientific Press, Wymondham, U.K. (in press).
21. Tang, J., and Breaker, R. R. (1997) *Chem. Biol. 4*, 453−459.
22. Soukup, G. A., and Breaker, R. R. (1999) *Proc. Natl. Acad. Sci. U.S.A. 96*, 3584−3589.
23. Burgstaller, P., and Famulok, M. (1994) *Angew. Chem., Int. Ed. Engl. 33*, 1084−1087.
24. Burke, D. H., and Gold, L. (1997) *Nucleic Acids Res. 25*, 2020−2024.
25. Jiang, F., Kumar, R. A., Jones, R. A., and Patel, D. J. (1996) *Nature 382*, 183−186.
26. Dieckmann, T., Suzuki, E., Nakamura, G. K., and Feigon, J. (1996) *RNA 2*, 628−640.
27. Patel, D. J., Suri, A. K., Jiang, F., Jiang, L., Fan, P., Kumar, R. A., and Nonin, S. (1997) *J. Mol. Biol. 272*, 645−664.
28. Genieser, H.-G., Butt, E., Bottin, U., Dostmann, W., and Jastorff, B. (1989) *Synthesis*, 53−54.
29. Ikehara, M., Kaneko, M., and Okano, R. (1970) *Tetrahedron 26*, 5675−5682.
30. Verheyden, J. P. H., and Moffatt, J. G. (1970) *J. Org. Chem. 35*, 2319−2326.
31. Breaker, R. R., and Joyce, G. F. (1994) *Trends Biotechnol. 12*, 268−275.
32. Tang, J., and Breaker, R. R. (1998) *Nucleic Acids Res. 26*, 4214−4221.
33. Zuker, M. (1989) *Science 244*, 48−52. The RNA *mfold* server can be accessed on the Internet (www.ibc.wustl.edu/∼zuker/rna/form1.cgi).
34. Soukup, G. A., and Breaker, R. R. (1999) *RNA 5*, 1308−1325.
35. Nadeau, J. G., Singleton, C. K., Kelly, G. B., Weith, H. L., and Gough, G. R. (1984) *Biochemistry 23*, 6153−6159.
36. Burke, D. H., and Hoffman, D. C. (1998) *Biochemistry 37*, 4653−4663.
37. Broom, A. D., Schweizer, M. P., and Ts'O, P. O. P. (1967) *J. Am. Chem. Soc. 89*, 3612−3622.
38. Saenger, W. (1984) in *Principles of Nucleic Acid Structure*, pp 69−78, Springer-Verlag, New York.
39. Watenpaugh, K., Dow, J., Jensen, L. H., and Furberg, S. (1968) *Science 159*, 206−207.
40. Fazakerley, G. V., Russell, J. C., and Wolfe, M. A. (1977) *Eur. J. Biochem. 76*, 601−605.
41. Sheldrick, W. S., and Rieke, E. (1978) *Acta Crystallogr. B34*, 2324−2327.
42. Abdallah, M. A., Biellman, J.-F., Nordstrom, B., and Branden, C.-I. (1975) *Eur. J. Biochem. 50*, 475−481.
43. Werstruck, G., and Green, M. R. (1998) *Science 282*, 296−298.
44. Araki, M., Okuno, Y., Hara, Y., and Sugiura, Y. (1998) *Nucleic Acids Res. 26*, 3379−3384.
45. Soukup, G. A., and Breaker, R. R. (1999) *Struct. Fold. Des. 7*, 783−791.
46. Koizumi, M., Soukup, G. A., Kerr, J. Q., and Breaker, R. R. (1999) *Nat. Struct. Biol.* 6, 1062−1071.

BI000149N